Aqueous Angiography–Mediated Guidance of Trabecular Bypass Improves Angiographic Outflow in Human Enucleated Eyes

Alex S. Huang,[1,2] Sindhu Saraswathy,[1] Anna Dastiridou,[1] Alan Begian,[2] Chirayu Mohindroo,[1] James C. H. Tan,[1,2] Brian A. Francis,[1,2] David R. Hinton,[3] and Robert N. Weinreb[4]

[1]Doheny Eye Institute, Los Angeles, California, United States
[2]Department of Ophthalmology, David Geffen School of Medicine at University of California-Los Angeles, Los Angeles, California, United States
[3]Department of Ophthalmology and Pathology, University of Southern California, Los Angeles, California, United States
[4]Hamilton Glaucoma Center and Shiley Eye Institute, University of California-San Diego, San Diego, California, United States

Correspondence: Alex Huang, Doheny Eye Institute, Department of Ophthalmology, David Geffen School of Medicine, University of California-Los Angeles, 1355 San Pablo Street, Los Angeles, CA 90033, USA; Ahuang@Doheny.org.

Submitted: March 27, 2016
Accepted: July 27, 2016

Citation: Huang AS, Saraswathy S, Dastiridou A, et al. Aqueous angiography–mediated guidance of trabecular bypass improves angiographic outflow in human enucleated eyes. *Invest Ophthalmol Vis Sci*. 2016;57:4558–4565. DOI: 10.1167/iovs.16-19644

Purpose. To assess the ability of trabecular micro-bypass stents to improve aqueous humor outflow (AHO) in regions initially devoid of AHO as assessed by aqueous angiography.

Methods. Enucleated human eyes (14 total from 7 males and 3 females [ages 52–84]) were obtained from an eye bank within 48 hours of death. Eyes were oriented by inferior oblique insertion, and aqueous angiography was performed with indocyanine green (ICG; 0.4%) or fluorescein (2.5%) at 10 mm Hg. With an angiographer, infrared and fluorescent images were acquired. Concurrent anterior segment optical coherence tomography (OCT) was performed, and fixable fluorescent dextrans were introduced into the eye for histologic analysis of angiographically positive and negative areas. Experimentally, some eyes ($n = 11$) first received ICG aqueous angiography to determine angiographic patterns. These eyes then underwent trabecular micro-bypass sham or stent placement in regions initially devoid of angiographic signal. This was followed by fluorescein aqueous angiography to query the effects.

Results. Aqueous angiography in human eyes yielded high-quality images with segmental patterns. Distally, angiographically positive but not negative areas demonstrated intrascleral lumens on OCT images. Aqueous angiography with fluorescent dextrans led to their trapping in AHO pathways. Trabecular bypass but not sham in regions initially devoid of ICG aqueous angiography led to increased aqueous angiography as assessed by fluorescein ($P = 0.043$).

Conclusions. Using sequential aqueous angiography in an enucleated human eye model system, regions initially without angiographic flow or signal could be recruited for AHO using a trabecular bypass stent.

Keywords: minimally invasive glaucoma surgery, aqueous angiography, imaging

Trabecular-targeted Minimally Invasive Glaucoma Surgeries (MIGS) offer a safe and fast option for intraocular pressure (IOP) lowering in glaucoma.[1,2] However, trabecular meshwork (TM) bypass or ablation MIGS demonstrate variable and inconsistent IOP lowering[3,4] that hinders greater adoption and wider use. Multiple hypotheses exist to explain this variability, including improper surgical placement within the TM as related to a surgical learning curve. Another hypothesis is that with segmental aqueous humor outflow (AHO), the surgeon has to place the surgery in the correct location 360° around the limbus to maximize IOP lowering.[5,6]

The definition of the optimal location is itself unclear for AHO and trabecular MIGS. Various methods have demonstrated that AHO is segmental and nonuniform circumferentially 360° around the limbus.[5,7–17] Even with this knowledge, it is unclear how segmental outflow impacts results of trabecular MIGS. In particular, it is not known if maximum IOP lowering would be achieved with performing trabecular bypass in regions of preoperatively better or worse AHO.

Aqueous angiography is a form of anterior segment fluorescent angiography[18] that is a real-time method to visualize AHO.[5] Aqueous angiography has been tested in multiple species with multiple tracers consistently demonstrating segmental patterns. Sequential aqueous angiography with indocyanine green (ICG) followed by fluorescein allows for testing interventions performed between the angiographies of the two tracers. Here, we used a greater number of model enucleated human eyes to better characterize AHO and aqueous angiography in humans. Then, we tested whether trabecular bypass using a trabecular bypass stent can improve AHO as measured by aqueous angiography. In particular, we tested if regions of initially poor AHO can be recruited for improvement.

Methods

Test Subjects

Ten humans (7 male and 3 female; ages 52–84) provided 14 postmortem eyes (8 right and 6 left) from the San Diego Eye

Investigative Ophthalmology & Visual Science

Bank within 48 hours of death. Listed causes of death included cancer (leukemia, esophageal, and myelodysplastic syndrome), dementia, failure to thrive, liver failure, gastrointestinal bleed, myocardial infarction, and urinary tract injection. No subject was known to have a history of glaucoma. To summarize the information below, dextran experiments used 2 eyes, OCT imaging used 1 eye, and trabecular bypass experiments used 11 eyes. Eyes were always received as pairs, but some eyes were excluded as they were either open globes due to inadvertent trauma during procurement by the eye bank or because fluid leaks developed during experimentation such that IOP was uncertain.

Aqueous Angiography

Aqueous angiography was performed as described before.[5] Eyes were trimmed of extraocular tissue, oriented by inferior oblique insertion location,[19] and pinned to Styrofoam. A Lewicky Anterior Chamber (AC) Maintainer (BVI Visitec, Alcester, UK) was inserted through a 1-mm side port (Alcon, Fort Worth, TX, USA) into the anterior chamber. Balanced salt solution (BSS; Alcon) was introduced for a 1-hour preperfusion period at room temperature (RT) with a reservoir height set at 5 inches above the eye to provide a gravity-delivered pressure of ~10 mm Hg as previously described. Eyes were kept moist with RT BSS-soaked gauze. Simultaneously, 25% fluorescein (Akorn, Lake Forest, IL, USA) was diluted at RT in BSS to 2.5%. Indocyanine green (ICG; I2633; Sigma-Aldrich Corp., St. Louis, MO, USA) was dissolved with water into a 2% stock solution, and ICG was subsequently diluted in BSS to 0.4%. These concentrations were chosen because they have been described for clinical use in live humans as intraocular capsular stains for cataract surgery.[20]

In most cases, ICG ($n = 11$) was first introduced for aqueous angiography at 10 mm Hg followed by fluorescein aqueous angiography in the same eye as previously done in cows (Saraswathy S, et al. *IOVS* 2015;56:ARVO E-Abstract 247). Alternatively, 3-kD fixable and fluorescent dextrans (Life Technologies, Carlsbad, CA, USA; diluted to 2.5 mg/mL in BSS) were used ($n = 2$) at 10 mm Hg.[5,21,22] The eyes were placed in front of the Spectralis HRA+OCT (Heidelberg Engineering, Heidelberg, Germany; fluorescein capture mode: excitation wavelength = 486 nm and transmission filter set at >500 nm; ICG capture mode: excitation wavelength = 786 nm and transmission filter set at >800 nm) with fluorescent images taken with a 55° lens using a 25-diopter focus. Confocal scanning laser ophthalmoscopic (cSLO) infrared images were taken to center the eye. Prior to tracer application, cSLO fluorescent angiographic images using the fluorescein or ICG capture mode were taken to provide a standard pretracer intensity background image, which appeared black. Subsequent fluorescein or ICG capture mode images were taken at various time points in various positions or face-on after tracer introduction. To prevent image signal intensity saturation over time during prolonged imaging sessions, the laser sensitivity setting on the Spectralis was adjusted with each image to set the central fluorescent signal in the anterior chamber to just under signal saturation.

Histologic Processing and Microscopy for Dextran Experiments

After aqueous angiography with fluorescent dextrans for ~2 minutes in human eyes ($n = 2$), the intracameral fluorescent dextran solution was exchanged with 4% paraformaldehyde (PFA) for 15 minutes at 10 mm Hg.[5] The entire globe was then placed in 4% PFA for an additional 15 minutes of fixation. Wedges including the angle were cut from angiographically positive and negative regions, dehydrated through ethanol steps, brought through xylenes, and paraffin embedded. Five-micrometer-thick sections were cut on a Leitz 1512 microtome (Leica Biosystems, Vista, CA, USA) onto Superfrost Plus slides (VWR, Radnor, PA, USA) and air dried. Sections were deparaffinized through xylenes and rehydrated through diminishing ethanol steps. Slides were mounted with a 4′,6-diamidino-2-phenylindole (DAPI)-containing mounting medium (Vector Labs, Burlingame, CA, USA) and viewed under a Keyence BZ-X700 digital imaging microscope (Keyence, Chicago, IL, USA). Sections were imaged using a ×4 Plan Fluor lens with a 0.13 numerical aperture. All images were taken using identical settings for illumination and image capture sensitivity (Keyence imaging software v.1.51). For FITC-dextrans (EX BP 470/30, DM 495, EM BP 520/35) and DAPI (EX BP 360/40, DM 400, EM BP 460/50), appropriate filters were used, respectively. Fluorescent quantitative analyses were completed similarly to those previously reported.[5] Briefly, fluorescence pixel intensity was determined in a region of interest centered on the angle (Photoshop CS5 v.12x32; Adobe, San Jose, CA, USA). Background-adjusted intensity values were obtained by subtracting the background in each image (by sampling empty anterior chamber) from the above fluorescence pixel intensity in each angle. Statistical comparison of the background-adjusted intensity values was conducted with 2-sample, equal-sized, unpaired, assumed normal variance Student's *t*-tests (Excel 2010; Microsoft, Redmond, WA, USA).

Trabecular Bypass Experiments

After the initial ICG aqueous angiography, regions with poor angiographic signal were marked and targeted for sham ($n = 5$) versus trabecular bypass stents ($n = 6$). Given the use of enucleated human eyes, the corneas were universally edematous, and despite various methods (epithelial debridement, corneal dehydration, and external transillumination), visualization of the TM for intervention through a gonioprism was not possible. Therefore, an alternative approach was devised whereby a full-thickness corneal incision was made with a 1-mm side-port blade perpendicular to the proposed stent/sham site approximately 80% of the limbal white-to-white distance in that meridian. Careful consideration was made not to include the wound of the 1-mm side port created for the Lewicky AC Maintainer. Balanced salt solution was irrigated into the anterior chamber to wash out ICG and improve visualization. Wek-Cel sponges (BVI Visitec, Alcester, UK) were used to remove excess fluid, and direct visualization of the angle and TM was made through a research-dedicated surgical microscope (Leica, Buffalo Grove, IL, USA). Sham treatment was achieved by touching the TM at the proposed site using an 18-gauge (g) blunt fill needle (BD, Franklin Lakes, NJ, USA). The anterior chamber was refilled with BSS and the corneal wound reapproximated with cyanoacrylate glue. Aqueous angiography was performed again with fluorescein. In one case, anterior segment OCT was taken over the region of stent placement (see below). All eyes were then placed in 4% PFA overnight at 4C°. The eyes were prepared for histologic sectioning after removal of the stent much as explained above with hematoxylin and eosin staining for evaluation of the angle at the stent/sham location.

Trabecular bypass was performed using trabecular bypass stents (provided by Glaukos Corporation, Laguna Hills, CA, USA). Trabecular bypass stents (generation 1, G1) are Food and Drug Administration (FDA) approved for combined cataract and glaucoma surgery for IOP lowering in cases of moderately advanced glaucoma.[2,4,23] To facilitate placement, second-generation stents (G2W; iStent Inject)[23–25] were used (Fig. 1). Second-generation stents are not currently FDA approved

Investigative Ophthalmology & Visual Science

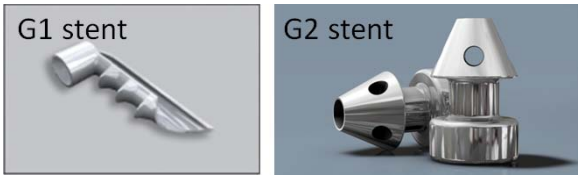

FIGURE 1. Trabecular micro-bypass stents. Trabecular bypass stents were provided by Glaukos Corporation for these experiments. The generation 1 (G1) stent is FDA approved for moderate glaucoma combined with cataract surgery. With the snorkel-like shape, the stent is inserted into the trabecular meshwork so that one lumen is in front of and the other lumen is behind the trabecular meshwork. This requires a sideways motion on insertion. Generation 2 (G2) stents (iStent inject) are non-FDA approved currently and were used for these experiments because of the mushroom shape whereby the stent is directly injected into and past the trabecular meshwork straight on, such that the mushroom head with side ports is past the trabecular meshwork while the posterior flat flange with central lumen is in communication with the anterior chamber. Images provided courtesy of Rob Liff, Glaukos Corporation.

and differ from G1 stents by shape and approach to theoretically allow for easier delivery. In these experiments, the handpiece of the G2W stent was advanced into the anterior chamber through the corneal wound until the trochar tip touched the TM at the proposed injection site. Depression of the injection button allowed forward delivery of the stent past the TM without the sideways motion required for G1 stents. Closure of the eye and subsequent fluorescein aqueous angiography were conducted as above for sham conditions.

Aqueous Angiography Image Processing

To quantify changes in angiographic signal from angle intervention or sham from each individual eye, ICG and fluorescein aqueous angiography intensity over time was determined as previously described.[5] Aqueous angiographic images were opened in Photoshop CS5 (v.12x32) for image processing and pixel intensity measurements. Both sham and experimental eyes were pooled for this purpose given the cost and precious nature of enucleated human eyes for research. Briefly, (1) angiographic signal within the anterior chamber and beyond the globe horizon for each eye was cropped out to create a total ring of angiographic data. (2) The background fluorescein angiography signal was then established by determining "average background pixel intensity" from a region of interest in the center of each eye from the pretracer image mentioned above. (3) Average pixel intensities for all rings were then obtained and background adjusted by subtracting out the "average background pixel intensity." (4) To control for manual adjustments to the Spectralis laser sensitivity settings during image acquisition, the background-adjusted average pixel intensity from each ring was divided by the numerical value on the Spectralis laser sensitivity setting to yield a normalized intensity value.

Quantitative assessments of the trabecular bypass experiments were then based on comparing ICG (3 minutes) and fluorescein (45 seconds) images at two time points that resided on relatively linear portions of their respective curves. Tracer-specific intensity over background values (TS-IOB) were calculated (Fig. 2). For each eye, pixel intensity was first measured using a 75 × 75-pixel test area that was placed over the region of interest next to the stent or sham treatment. This value was divided by another pixel intensity measure taken from a clearly signal-poor region from the same eye to determine the ratio of signal intensity of the region of interest (next to the treatment area) over background signal in each eye. The influence of the sham or trabecular bypass was then

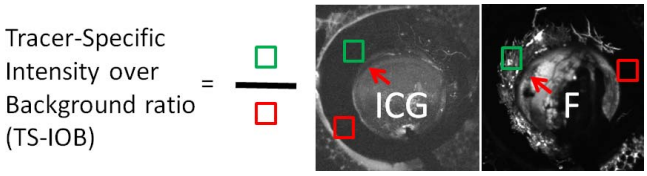

FIGURE 2. Tracer-specific intensity over background ratio (TS-IOB). To quantify the change in angiographic outflow for each eye, the perilimbal signal intensity adjacent to the area of intervention (sham or stent; *red arrows*) was recorded (*green box*) and divided by a region of interest (*red box*) in a clearly signal-poor region in the exact same image to calculate a tracer-specific (indocyanine green [ICG] or fluorescein [F]) intensity over background ratio.

determined by dividing TS-IOB (fluorescein) by TS-IOB (ICG). Values around 1 would imply no change. Statistical comparisons between sham and stent were conducted with 2-sample, equal-sized, unpaired, assumed normal variance Student's *t*-tests.

Anterior Segment Optical Coherence Tomography (OCT)

Anterior segment OCT (anterior segment module [Heidelberg Engineering] on Scleral mode) was concurrently conducted in one eye with ICG aqueous angiography alone to determine if angiographically positive regions showed vessel anatomy compatible for AHO. Single line scans with a 15° scan angle (3.9-μm axial and 11-μm lateral resolution; ~4.5 mm) were taken with oversampling (automated real-time [ART] = 20) in angiographically positive/negative regions.

Anterior segment OCT was also performed in one case of stent placement as mentioned above. Here a volume scan was taken with a Heidelberg Engineering–provided custom script near the area of stent placement (15° × 2.5° scan angle; 128 B-scans; axial/lateral resolution of 3.8/11 μm, respectively, B-scan to B-scan distance of 11 μm).

Video

The anterior segment OCT images in one of the stent cases were exported as a video per manufacturer instructions on the Spectralis. Images were opened in Photoshop and brightness/contrast adjusted to enhance visualization of particulate debris located in the anterior chamber. All images were treated equally. The presence of this debris was likely secondary to the act of the trabecular bypass/sham procedure itself.

RESULTS

Aqueous Angiography in Human Eyes Represents Aqueous Humor Outflow (AHO)

As in pigs,[5] aqueous angiography in human enucleated model eyes demonstrated segmental angiographic signal that reflected AHO as evaluated by fluorescent dextran (Fig. 3) and OCT experiments (Fig. 4). Visual inspection of the initial aqueous angiography in all 14 eyes (regardless of what tracers was used first [fluorescein, ICG, or fluorescent dextrans]) showed that 11/14 eyes (78.6%) had predominately nasal angiographic signal.

To look for differences in outflow in the TM and angle region, we used fixable and trappable dextrans. While unlikely imaging the TM itself in aqueous angiography, TM near-adjacent positive but not negative aqueous angiographic signal demonstrated trapping of the dextrans in AHO pathways (Figs. 3B, 3E [green lines from Figs. 3A, 3D] versus Figs. 3C, 3F [red lines from Figs. 3A, 3D]). Note similar nonspecific fluorescence of Descemet's

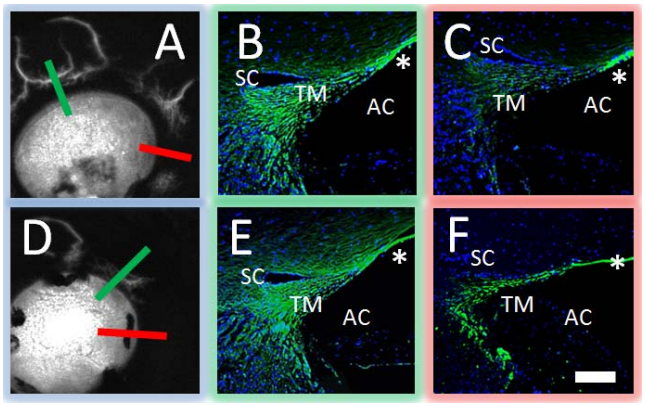

Figure 3. Aqueous angiography localized to AHO pathways in human eyes. Aqueous angiography was performed with 3-kD fixable fluorescent dextrans in human eyes. Two separate eyes (**A–C**, **D–F**) are shown here. Angiographically positive (**A**, **D**; *green lines*) or diminished (**A**, **D**; *red lines*) regions were identified with aqueous angiography, marked, and prepared for paraffin sectioning. In the first eye (**A–C**), angiographically positive areas (*green line* in [**A**] corresponds to [**B**]) showed greater trapping of dextrans within outflow pathways compared to angiographically diminished (*red line* in [**A**] corresponds to [**C**]) regions. In the second eye (**D–F**), angiographically positive areas (*green line* in [**D**] corresponds to [**E**]) also showed more trapping of dextrans in outflow pathways compared to angiographically diminished (*red line* in [**D**] corresponds to [**F**]) regions. Note similar degree of nonspecific fluorescence seen in Descemet's membrane in all cases (*asterisks*). SC, Schlemm's canal; TM, trabecular meshwork; AC, anterior chamber. *Scale bar*: 100 μm.

membrane in all conditions (Fig. 3; asterisks). Quantitative comparison of background-adjusted intensity values in angiographically positive compared to negative areas showed a statistically significant increase (100.76 ± 18.52 vs. 34.19 ± 13.21; background-adjusted intensity units; average ± SD; $n=12$ sections for each condition; $P < 0.001$ 2-tailed Student's *t*-test).

Anterior segment OCT supported dextran results where ICG angiographically positive but not negative areas showed intrascleral lumens reminiscent of AHO pathways (Fig. 4).

Aqueous Angiography and Trabecular Bypass Experiments

To assess whether trabecular bypass could improve regions of poor aqueous angiography signal, sequential aqueous angiography with ICG followed by fluorescein was performed. Areas of poor ICG aqueous angiography signal were marked (Figs. 5, 6; red arrows), and full-thickness cornea incisions were made for direct visualization of the TM for a sham treatment (Fig. 5; $n = 5$) (touching the TM with a blunt-tip 18-g needle) or trabecular bypass (Fig. 6; $n = 6$ [of which 5 achieved full-thickness bypass]) with a trabecular bypass stent. Corneal wounds were glued, and fluorescein aqueous angiography was performed to assess the influence of the intervention. For both sham and stent conditions (Figs. 5, 6) green arrows demonstrated similar aqueous angiography patterns between ICG and fluorescein. After sham, regions initially devoid of ICG aqueous angiography signal continued to be so with fluorescein aqueous angiography (Fig. 5). However, after trabecular bypass, regions initially devoid of ICG aqueous angiography signal demonstrated qualitative increased aqueous angiography signal intensity with fluorescein (Fig. 6).

Histologic sectioning in marked areas after sham treatment demonstrated normal-appearing TM and angle structures (Fig. 7). Histologic sections of marked areas after trabecular bypass demonstrated successful and full-thickness TM ablation (Figs. 8A–C). This was confirmed noninvasively with anterior segment OCT in one case (Fig. 8D). Interestingly, one case occurred in which after attempted trabecular bypass, only minimally improved fluorescent aqueous angiographic signal was seen with fluorescein (Fig. 9). Histology in that case showed unsuccessful stent placement whereby the TM was only partially bypassed (Fig. 9).

Given the universally edematous corneas in all eyes, a modified surgical approach was developed in the sham and stent experiments. Full-thickness corneal wounds, longer than routinely used for clinical surgeries in patient care, were employed, and irrigation using BSS was required to wash out fluorescent tracers to directly visualize the TM. Therefore, debris was found in some cases in the anterior chamber after stent placement. In one eye (Figs. 6A–H) that had stent placement in an initially ICG aqueous angiography–poor region with additional histology and OCT-confirmed successful trabecular bypass stent placement (Figs. 8A–D), an OCT volume scan was taken. Video demonstration of these scans showed particulate matter flowing toward the trabecular bypass stent (Supplementary Video S1).

To quantify aqueous angiographic changes in trabecular bypass experiments, experimental and sham eyes were pooled and total intensity of ICG and fluorescein aqueous angiographic signal plotted over time (Fig. 10). Not unlike what was shown in a previous report,[5] there was a steady increase.

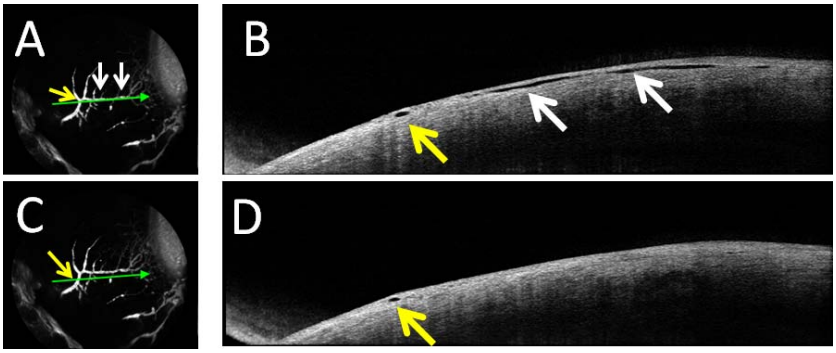

Figure 4. Aqueous angiography and optical coherence tomography (OCT) in a human eye. Indocyanine green (ICG) aqueous angiography was conducted concurrent with anterior segment OCT focused on the distal angiographic signal from the right eye of an 84-year-old male (listed cause of death, myelodysplastic syndrome). (**A**) Angiographically positive regions (*yellow arrow* and *white arrows*) demonstrated (**B**) intrascleral lumens compatible with aqueous humor outflow on OCT. (**C**) In an OCT B-scan taken directly below the angiographic signal depicted in (**A**), (**D**) intrascleral lumens were mostly absent. (**C**) This is true except one for one point on the *left* of the angiographic image (*yellow arrow*) where the OCT image caught one branch of the angiographic pattern that (**D**) showed a single oval corresponding intrascleral lumen on OCT.

Investigative Ophthalmology & Visual Science

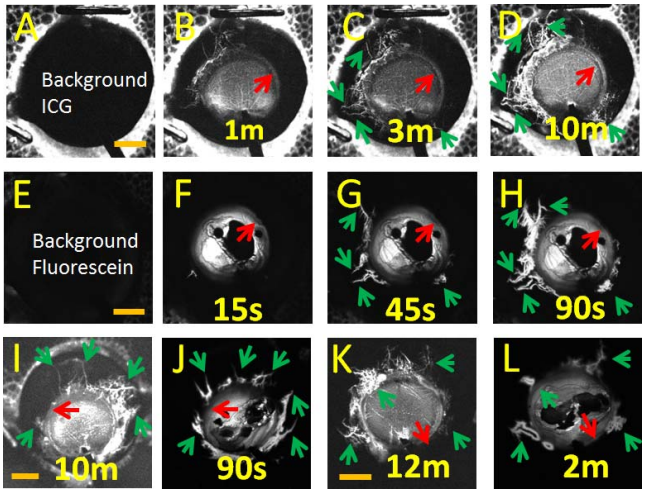

Figure 5. Sequential aqueous angiography with indocyanine green (ICG) followed by fluorescein after sham intervention to the trabecular meshwork. (**A–D**) ICG aqueous angiography was first performed on the left eye of a 68-year-old male (listed cause of death, failure to thrive). This was followed by identification of a region of low signal (*red arrows*), full-thickness corneal incision perpendicular to this site, sham touch of the trabecular meshwork by an 18-g blunt needle, and cyanoacrylate glue closure of the wound. (**E–H**) This procedure was followed by fluorescein aqueous angiography in the same eye demonstrating continued poor angiography signal at the sham site (*red arrows*). (**A–H**) *Green arrows* demonstrate similar angiographic patterns between ICG and fluorescein outside of the sham location. (**I**, **J**) Representative images from ICG and fluorescein aqueous angiography from the right eye of a 76-year-old male (listed cause of death, myocardial infarction). (**K**, **L**) Representative images from ICG and fluorescein aqueous angiography from the left eye of the same 76-year-old male (listed cause of death, myocardial infarction). All images were arranged such that superior is on *top*, and inferior is on the *bottom* of the image. For right eyes, nasal is on the *right* of the image, and temporal is on the *left*. The opposite is true for left eyes. Background, pretracer application fluorescent image; m, minutes; s, seconds. *Orange scale bars*: 5 mm.

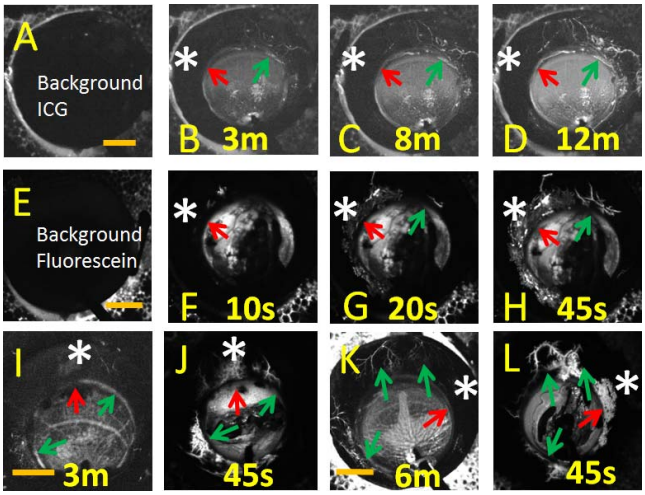

Figure 6. Sequential aqueous angiography with indocyanine green (ICG) followed by fluorescein after trabecular bypass stent placement. (**A–D**) ICG aqueous angiography was first performed on the right eye of a 79-year-old male (listed cause of death, esophageal cancer). This was followed by identification of a region of low signal (*red arrows* and *white asterisks*), full-thickness corneal incision perpendicular to this site, placement of a second-generation trabecular bypass stent under direct visualization, and cyanoacrylate glue closure of the wound. (**E–H**) This procedure was followed by fluorescein aqueous angiography in the same eye demonstrating earlier and increased angiographic signal compared to before the stent placement (*red arrows* and *white asterisks*). (**A–H**) *Green arrows* demonstrate similar angiographic patterns between ICG and fluorescein in regions outside of stent placement. (**I**, **J**) Representative images from ICG and fluorescein aqueous angiography from the right eye of an 82-year-old female (listed cause of death, urinary tract infection). (**K**, **L**) Representative images from ICG and fluorescein aqueous angiography from the left eye of a 75-year-old female (listed cause of death, dementia). All images were arranged such that superior is on *top*, and inferior is on the *bottom* of the image. For right eyes, nasal is on the *right* of the image, and temporal is on the *left*. The opposite is true for left eyes. Background, pretracer application fluorescent image; m, minutes; s, seconds. *Orange scale bars*: 5 mm.

To assess for regional changes in angiographic patterns after sham or stent, TS-IOB ratios were calculated for ICG and fluorescein images at 3 minutes and 45 seconds, respectively (Fig. 2). These time points were chosen based on their positions at early and linear portions of each tracer's respective curves (Figs. 10E–F). After dividing fluorescein TS-IOB over ICG TS-IOB for sham and stent conditions, a statistically significant improvement was found for the stent trabecular bypass condition (sham [$n = 5$]: 1.02 ± 0.46 versus stent [$n = 5$]: 17.37 ± 7.76; $P = 0.043$). Interestingly, in the one case of partial TM bypass (Fig. 9), an intermediate value of fluorescein TS-IOB over ICG TS-IOB (1.66) was seen.

Discussion

Segmental patterns of angiographic AHO were observed in human eyes. Optical coherence tomography evaluation of distal aqueous angiography signal showed episcleral lumens compatible with AHO in angiographically positive but not negative regions. With sequential aqueous angiography, the effect of trabecular bypass was tested. In these studies, the sole manipulation of trabecular bypass improved AHO as measured by fluorescein aqueous angiography in areas initially devoid of ICG aqueous angiography. These results are interesting for several reasons.

First, the meaning of aqueous angiography in this model system is limited by the fact that the eyes are enucleated. Artifacts due to diminished cell viability and episcleral venous blood clotting could affect angiographic patterns. In particular, postmortem presence of distal episcleral venous blood clots could explain segmental patterns by sectorally blocking AHO. However, since TM bypass alone resulted in improved aqueous angiography signal, segmental AHO as seen by aqueous angiography could not be entirely and artifacticiously due to episcleral venous clots since these clots would reside distal to the TM.

Also, depth must also be considered when viewing differences in angiographic signal. Lack of angiographic signal

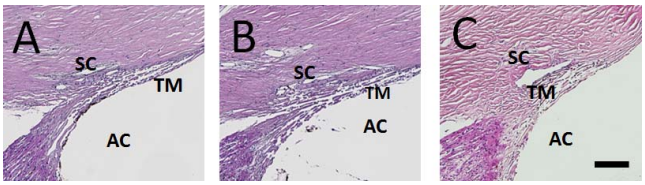

Figure 7. Trabecular meshwork after sham experiments. (**A–C**) After sham experiments, eyes were perfusion fixed and the anterior segments prepared for paraffin sectioning and hematoxylin/eosin staining demonstrating intact trabecular meshwork. (**A**) The same eye as in Figures 5A through 5H. (**B**) The same eye as in Figures 5I and 5J. (**C**) The same eye as in Figures 5K and 5L. SC, Schlemm's canal; TM, trabecular meshwork; AC, anterior chamber. *Scale bar*: 100 μm.

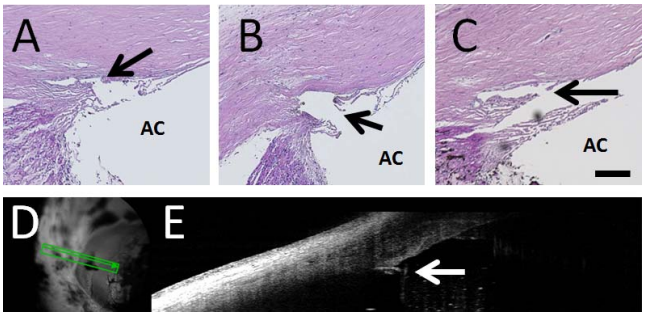

FIGURE 8. Trabecular meshwork after trabecular bypass stent experiments. (**A**–**C**) After trabecular bypass stent experiments, eyes were perfusion fixed and the anterior segments prepared for paraffin sectioning and hematoxylin/eosin staining. *Arrows* point out successful full-thickness trabecular bypass in all cases. (**A**) The same eye as in Figures 6A through 6H. (**B**) The same eye as in Figures 6I and 6J. (**C**) The same eye as in Figures 6K and 6L. (**D**) Anterior segment optical coherence tomography in the same eye as in Figures 6A through 6H and Figure 8A demonstrated correct positioning of trabecular bypass stent. AC, anterior chamber. *Scale bar*: 100 μm.

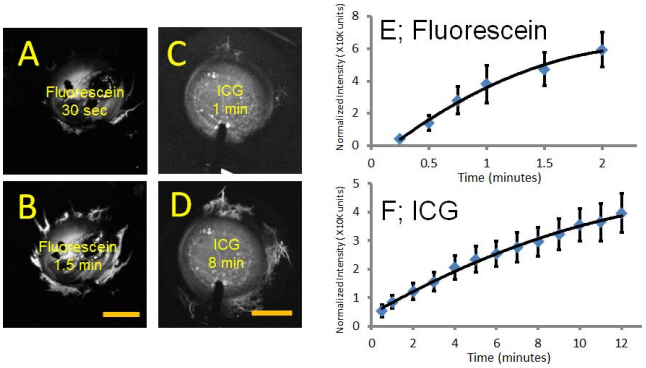

FIGURE 10. Aqueous angiography signal intensity rose over time in human eyes. (**A**, **B**) Aqueous angiography with fluorescein over time demonstrated accumulated signal intensity. (**C**, **D**) Aqueous angiography with indocyanine green (ICG) over time also demonstrated accumulated signal intensity. Total normalized pixel intensity values from 11 eyes each for (**E**) fluorescein and (**F**) ICG were recorded as a function of time at 10 mm Hg. ICG demonstrated a slower and smaller rise in signal intensity consistent with previous report. Graphs show mean ± standard error. *Orange scale bars*: 5 mm.

could be due to outflow pathways diving deep into the sclera such that excitation/emission wavelengths become attenuated. Since TM bypass alone, which did not influence the sclera or scleral depth, resulted in improved angiographic signal, segmental AHO could not be entirely due to issues of depth. Additionally, depth influences interpretation of aqueous angiography results. Increased depth can attenuate light transmission through sclera; and given the location where angiographic signal appears perilimbal but also posterior to the limbus, aqueous angiography signal represents the outflow result as influenced by the entire trabecular outflow pathway without directly imaging the TM. This is in contrast to microsphere or bead methods, which have the advantage of demonstrating precise segmental TM AHO but used tissue processing not compatible with live imaging.[7–17]

Second, improving AHO by ablating the TM reemphasizes to clinicians and scientists the importance of the TM. Variable results of clinical TM ablation/bypass MIGS naturally raised the possibility of outflow obstruction in the distal outflow pathways.[6] While distal AHO is likely relevant and a source of undiscovered biology and potential disease, the results of improved angiographic AHO by only trabecular bypass

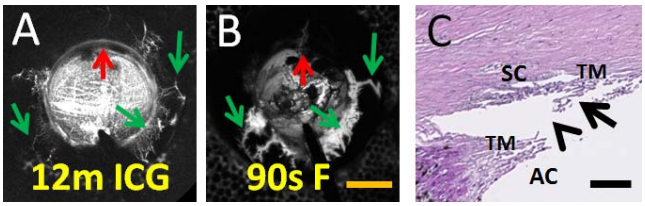

FIGURE 9. Aqueous angiography with partial trabecular bypass. (**A**) Sequential aqueous angiography was performed in the right eye of a 75-year-old female (listed cause of death, dementia), first with ICG showing lack of signal superior (*red arrow*) even after a prolonged time period. This was followed by trabecular bypass stent placement. (**B**) Subsequent fluorescein aqueous angiography barely demonstrated improved angiographic outflow signal (*red arrow*). (**C**) Histologic sectioning over the stent placement site showed a cleft where the stent resided (*arrowhead*) with only partial TM bypass without full-thickness bypass achieved (*arrow*). All images were arranged such that superior is on *top* and inferior is on the *bottom* of the image. In this right eye, nasal is on the *right* of the image, and temporal is on the *left*. SC, Schlemm's canal; TM, trabecular meshwork; AC, anterior chamber. *Orange scale bar*: 5 mm. *Black scale bar*: 100 μm.

reinforces the role of the TM in gating AHO.[26,27] Also, the result of diminished AHO improvement with partial TM bypass is important (Fig. 9). Part of the variable clinical results from trabecular MIGS may come from improper surgical placement. A natural learning curve exists for all surgeries, and trabecular MIGS are no different.

Third, improving AHO in regions initially devoid of AHO expands on initial surgical approaches to MIGS. Trabecular MIGS are typically placed in the nasal angle through a temporal clear cornea direction[2,3] for several reasons. Ophthalmologists are accustomed to this approach because of phacoemulsification. Second, reports, including results here, suggest that AHO is normally best nasal.[28] Therefore, nasal MIGS placement was conducted to attempt access of these AHO pathways. However, if AHO is already adequate in a particular region, it is possible that trabecular bypass to enhance AHO in that region may limit further improvement due to a ceiling effect. Alternatively, another approach is to place trabecular MIGS where AHO is initially poor in an attempt to recruit these regions from a worse starting point. However, a counterargument to conducting MIGS in this way is that maybe the reason why AHO was diminished in the first place was that the local region never had adequate outflow channels to support AHO. This would be analogous to opening roads for vehicle traffic that ended up all being cul de sacs. Therefore, demonstrating that regions of poor AHO could be recruited for improved outflow opens the possibility of alternative surgical techniques. It is possible that better IOP lowering could be achieved by placing trabecular MIGS in regions of initially low AHO. Methods such as aqueous angiography now allow ophthalmologists to test the effects of various surgical approaches such as these. Additional testing needs to be done to attempt measurement of outflow facility concurrent with angiographic imaging. To do this, an aqueous humor dynamics rig will have to be situated and built around this clinical device as the center. With this, one could then test trabecular bypass in low versus high angiographic signal regions to determine if trabecular bypass in one area or the other really is better. Definite assessment will also require testing in clinical patients.

In the future, further studies need to be conducted with aqueous angiography in live humans and animals to avoid the confounding factors related to using enucleated eyes. For example, in cases of successful trabecular bypass, the increase in fluorescein aqueous angiography was variable, with some

cases rivaling native fluorescein angiographic signal in high-flow areas and in other cases to a lesser extent. This may have been due to either postmortem changes to distal outflow pathways giving a variable response to outflow recruitment for forward flow after trabecular bypass. Alternatively, subtle native differences in distal outflow anatomy between different low-flow regions being accessed could have created this variability as well.

Additionally, while the aqueous angiography patterns and time course between fluorescein and ICG were similar, they were not identical. This was likely secondary to differences in molecular properties (e.g., pH, molecular weight, protein binding). For example, the ICG signal was slower, and we speculate that this could be due to lower concentration used (ICG solubility is limited) or to the fact that ICG was more protein bound such that ICG aqueous angiography may model protein more than water movement. Despite being limited in these experiments to fluorescein and ICG by our commercial angiographer, given similar enough patterns and measurement of angiographic signal over specific regions of interest normalized for each dye with a TS-IOB ratio, we felt that methods for comparison were sufficient. From a laboratory standpoint, finer biochemical and molecular studies are planned that compare regions of initially greater or lesser AHO to develop a better understanding of what causes more or less AHO.

As AHO is better visualized through methods like aqueous angiography and more clinical experience with trabecular MIGS is gained, a better understanding of AHO will arise and improved questions can be asked. Ultimately, AHO imaging may allow for improved glaucoma surgical results or facilitate development of novel pharmacologic or surgical treatments.

Acknowledgments

Supported by National Institutes of Health, Bethesda, Maryland (K08EY024674 [ASH]); American Glaucoma Society (AGS) Mentoring for Physician Scientists Award 2013 [ASH] and 2014 [ASH]; AGS Young Clinician Scientist Award 2015 [ASH]; Research to Prevent Blindness Career Development Award 2016 [ASH]; and an unrestricted grant from Research to Prevent Blindness (New York, NY). The funders had no role in study design, data collection and analysis, decision to publish, or preparation of the manuscript.

Disclosure: **A.S. Huang**, Glaukos Corporation (F), Heidelberg Engineering (F); **S. Saraswathy**, None; **A. Dastiridou**, None; **A. Begian**, None; **C. Mohindroo**, None; **J.C.H. Tan**, None; **B.A. Francis**, None; **D.R. Hinton**, None; **R.N. Weinreb**, None

References

1. Richter GM, Coleman AL. Minimally invasive glaucoma surgery: current status and future prospects. *Clin Ophthalmol*. 2016;10:189–206.
2. Craven ER. Trabecular micro-bypass shunt (iStent®): basic science clinical, and future. *Middle East Afr J Ophthalmol*. 2015;22:30–37.
3. Minckler D, Mosaed S, Dustin L, Francis B; for the Trabectome Study Group. Trabectome (trabeculectomy-internal approach): additional experience and extended follow-up. *Trans Am Ophthalmol Soc*. 2008;106:149–159; discussion 159–160.
4. Craven ER, Katz LJ, Wells JM, Giamporcaro JE. Cataract surgery with trabecular micro-bypass stent implantation in patients with mild-to-moderate open-angle glaucoma and cataract: two-year follow-up. *J Cataract Refract Surg*. 2012;38:1339–1345.
5. Saraswathy S, Tan JC, Yu F, et al. Aqueous angiography: real-time and physiologic aqueous humor outflow imaging. *PLoS One*. 2016;11:e0147176.
6. Swaminathan SS, Oh DJ, Kang MH, Rhee DJ. Aqueous outflow: segmental and distal flow. *J Cataract Refract Surg*. 2014;40:1263–1272.
7. Swaminathan SS, Oh DJ, Kang MH, et al. Secreted protein acidic and rich in cysteine (SPARC)-null mice exhibit more uniform outflow. *Invest Ophthalmol Vis Sci*. 2013;54:2035–2047.
8. Braakman ST, Read AT, Chan DW, Ethier CR, Overby DR. Colocalization of outflow segmentation and pores along the inner wall of Schlemm's canal. *Exp Eye Res*. 2015;130:87–96.
9. Chang JY, Folz SJ, Laryea SN, Overby DR. Multi-scale analysis of segmental outflow patterns in human trabecular meshwork with changing intraocular pressure. *J Ocul Pharmacol Ther*. 2014;30:213–223.
10. Sabanay I, Gabelt BT, Tian B, Kaufman PL, Geiger B. H-7 effects on the structure and fluid conductance of monkey trabecular meshwork. *Arch Ophthalmol*. 2000;118:955–962.
11. Battista SA, Lu Z, Hofmann S, Freddo T, Overby DR, Gong H. Reduction of the available area for aqueous humor outflow and increase in meshwork herniations into collector channels following acute IOP elevation in bovine eyes. *Invest Ophthalmol Vis Sci*. 2008;49:5346–5352.
12. Ethier CR, Chan DW. Cationic ferritin changes outflow facility in human eyes whereas anionic ferritin does not. *Invest Ophthalmol Vis Sci*. 2001;42:1795–1802.
13. Keller KE, Bradley JM, Vranka JA, Acott TS. Segmental versican expression in the trabecular meshwork and involvement in outflow facility. *Invest Ophthalmol Vis Sci*. 2011;52:5049–5057.
14. Lu Z, Overby DR, Scott PA, Freddo TF, Gong H. The mechanism of increasing outflow facility by rho-kinase inhibition with Y-27632 in bovine eyes. *Exp Eye Res*. 2008;86:271–281.
15. Yang CY, Liu Y, Lu Z, Ren R, Gong H. Effects of Y27632 on aqueous humor outflow facility with changes in hydrodynamic pattern and morphology in human eyes. *Invest Ophthalmol Vis Sci*. 2013;54:5859–5870.
16. Vranka JA, Bradley JM, Yang YF, Keller KE, Acott TS. Mapping molecular differences and extracellular matrix gene expression in segmental outflow pathways of the human ocular trabecular meshwork. *PLoS One*. 2015;10:e0122483.
17. Cha ED, Xu J, Gong L, Gong H. Variations in active outflow along the trabecular outflow pathway. *Exp Eye Res*. 2016;146:354–360.
18. Marvasti AH, Berry J, Sibug Saber ME, Kim JW, Huang AS. Anterior segment scleral fluorescein angiography in the evaluation of ciliary body neoplasm: two case reports. *Case Rep Ophthalmol*. 2016;7:30–38.
19. Eagle R. Eye Pathology: An Atlas and Text. 2nd ed. Philadelphia: Lippincott Williams and Wilkins; 2001:291.
20. Jacobs DS, Cox TA, Wagoner MD, Ariyasu RG, Karp CL. Capsule staining as an adjunct to cataract surgery: a report from the American Academy of Ophthalmology. *Ophthalmology*. 2006;113:707–713.
21. Lindsey JD, Weinreb RN. Identification of the mouse uveoscleral outflow pathway using fluorescent dextran. *Invest Ophthalmol Vis Sci*. 2002;43:2201–2205.
22. Lindsey JD, Hofer A, Wright KN, Weinreb RN. Partitioning of the aqueous outflow in rat eyes. *Invest Ophthalmol Vis Sci*. 2009;50:5754–5758.
23. Klamann MK, Gonnermann J, Pahlitzsch M, et al. iStent inject in phakic open angle glaucoma. *Graefes Arch Clin Exp Ophthalmol*. 2015;253:941–947.
24. Bahler CK, Hann CR, Fjield T, Haffner D, Heitzmann H, Fautsch MP. Second-generation trabecular meshwork bypass stent (iStent inject) increases outflow facility in cultured

human anterior segments. *Am J Ophthalmol*. 2012;153: 1206–1213.

25. Voskanyan L, Garcia-Feijoo J, Belda JI, Fea A, Junemann A, Baudouin C. Prospective, unmasked evaluation of the iStent® inject system for open-angle glaucoma: synergy trial. *Adv Ther*. 2014;31:189–201.
26. Overby DR, Stamer WD, Johnson M. The changing paradigm of outflow resistance generation: towards synergistic models of the JCT and inner wall endothelium. *Exp Eye Res*. 2009;88: 656–670.
27. Johnson M. What controls aqueous humour outflow resistance? *Exp Eye Res*. 2006;82:545–557.
28. Johnstone M, Jamil A, Martin E. Aqueous veins and open angle glaucoma. In: Schacknow PN, Samples JR, eds. *The Glaucoma Book: A Practical, Evidence-Based Approach to Patient Care*. New York: Springer; 2010:65–78.

Investigative Ophthalmology & Visual Science